Icarus 274 (2016) 83–98

Contents lists available at ScienceDirect

Icarus

journal homepage: www.elsevier.com/locate/icarus

Planetary and satellite three body mean motion resonances

Tabaré Gallardo*, Leonardo Coito, Luciana Badano

Departamento de Astronomía, Instituto de Física, Facultad de Ciencias, Universidad de la República, Iguá 4225, 11400 Montevideo, Uruguay

ARTICLE INFO

Article history:
Received 3 January 2016
Revised 17 March 2016
Accepted 20 March 2016
Available online 31 March 2016

Keywords:
Celestial mechanics
Planetary dynamics
Resonances
Orbital
Satellites
Dynamics

ABSTRACT

We propose a semianalytical method to compute the strengths on each of the three massive bodies participating in a three body mean motion resonance (3BR). Applying this method we explore the dependence of the strength on the masses, the orbital parameters and the order of the resonance and we compare with previous studies. We confirm that for low eccentricity low inclination orbits zero order resonances are the strongest ones; but for excited orbits higher order 3BRs become also dynamically relevant. By means of numerical integrations and the construction of dynamical maps we check some of the predictions of the method. We numerically explore the possibility of a planetary system to be trapped in a 3BR due to a migrating scenario. Our results suggest that capture in a chain of two body resonances is more probable than a capture in a pure 3BR. When a system is locked in a 3BR and one of the planets is forced to migrate the other two can react migrating in different directions. We exemplify studying the case of the Galilean satellites where we show the relevance of the different resonances acting on the three innermost satellites.

1. Introduction

One of the most prevalent dynamical phenomena observed in planetary systems is orbital commensurability, or resonance. Two body resonances (2BRs), extensively studied in orbital dynamics, occur when the ratio between the mean motions, n, of two bodies can be written as a fraction of 2 small integer numbers. They have proven to be very important in the architecture of the planetary systems (Batygin, 2015; Fabrycky et al., 2014). A less common case of resonance ensues when the mean motions of three bodies P_0, P_1 and P_2 verify

$$k_0 n_0 + k_1 n_1 + k_2 n_2 \simeq 0 \tag{1}$$

being k_i small integers, generating which is called a three body resonance (3BR). In some cases, the 3BRs can be the consequence of a chain of two 2BRs as is the case of the Galilean satellites studied since Laplace. In fact, the three innermost Galilean satellites, Io, Europa and Ganymede, verify the 2BR relations $n_I - 2n_E \sim 0$ and $n_E - 2n_G \sim 0$. Subtracting both expressions we obtain the 3BR $n_I - 3n_E + 2n_G \sim 0$, called Laplacian resonance. The resulting dynamics it is not a mere addition of the two 2BRs and the emerging 3BR generates a new complex dynamics. The Laplacian resonance is a paradigmatic case of a 3BR generated by the superposition or chains of two 2BRs. On the other hand, there are also 3BRs that cannot be decomposed as chains of 2BRs and we will call them *pure*. Thousands of asteroids in pure 3BRs with Jupiter and Saturn can be found in the Solar System (Smirnov and Shevchenko, 2013).

A relevant parameter of the 3BRs is the order defined as $q = |k_0 + k_1 + k_2|$. It is known that the lower the order the larger the dynamical effects of the resonance. That is why between the Galilean satellites the dominant 3BR is $n_I - 3n_E + 2n_G \sim 0$, and not for example $n_I - n_E - 2n_G \sim 0$ which is of order 2 and obtained adding the 2BRs instead of subtracting them. Note that the resonant condition (1) can be written as

$$k_1(n_1 - n_0) + k_2(n_2 - n_0) + (k_0 + k_1 + k_2)n_0 \simeq 0 \tag{2}$$

which means that for zero order resonances, even in the case of pure 3BRs, the planets P_1 and P_2 are in a simple 2BR k_1:k_2 when looked from the rotating frame of the planet P_0. No other 3BRs have this property which makes zero order 3BRs a special case. Then, it is not surprising that zero order 3BRs have been deserved most the attention. They were studied for example by Aksnes (1988) who obtained general formulae with applications in the asteroid belt and systems of satellites. The case of Laplacian resonance in the Galilean satellites has been intensely studied (Ferraz-Mello, 1979; Lainey et al., 2009; Malhotra, 1991; Peale and Lee, 2002; Showman and Malhotra, 1997; Showman et al., 1997; Sinclair, 1975). Superposition or chains of 2BRs were also studied in the major Saturnian satellites (Callegari and Yokoyama, 2010) and in extrasolar systems (Batygin et al., 2015; Batygin and Morbidelli, 2013; Libert and Tsiganis, 2011; Martí et al., 2013; Papaloizou, 2015). Quillen and French (2014) focused on systems with

* Corresponding author. Tel.: +598 25258618.
E-mail address: gallardo@fisica.edu.uy, tabarega@gmail.com (T. Gallardo).

http://dx.doi.org/10.1016/j.icarus.2016.03.018
0019-1035/

close orbits with applications to the inner Uranian satellites, where it is remarked that 3BRs as consequence of superposition of first order 2BRs are the strongest ones. On the other hand, pure 3BRs were studied for example by Lazzaro et al. (1984) for the specific case of the Uranian satellites and by Nesvorný and Morbidelli (1999) where a complete planar theory was developed for the asteroidal, massless, case. The situation among the outer planets of the Solar System was analyzed numerically by Guzzo (2005); 2006). Quillen (2011) developed an analytical theory for general zero order resonances between three massive bodies in very close orbits while Gallardo (2014) developed a semianalytical method for estimation of the resonance's strength for pure 3BRs of any order for the asteroidal case assuming the perturbing planets in circular and coplanar orbits and the asteroid in an arbitrary orbit. Finally, it is worth mention that Showalter and Hamilton (2015) suggested that the satellites of Pluto, Styx, Nix and Hydra, are driven by the zero order 3BR $3n_S - 5n_N + 2n_H \sim 0$.

1.1. Looking for the disturbing function

The dynamics of a system trapped in a 3BR is determined by the resonant disturbing function, which its obtention is not a trivial point. The disturbing function for a 3BR emerges after a second averaging procedure applied on the resulting expressions of a first averaging involving the mutual perturbations between the planets taken by pairs (Nesvorný and Morbidelli, 1999). The final expression of the resonant disturbing function for planet P_0 assumed in the resonance given by Eq. (1) is a summatory of the type

$$\mathcal{R} = k^2 m_1 m_2 \sum_j \mathcal{P}_j \cos(\sigma_j) \tag{3}$$

where k is the Gaussian constant and m_1 and m_2 the planetary masses, with the critical angle

$$\sigma_j = k_0\lambda_0 + k_1\lambda_1 + k_2\lambda_2 + \gamma_j \tag{4}$$

and

$$\gamma_j = k_3\varpi_0 + k_4\varpi_1 + k_5\varpi_2 + k_6\Omega_0 + k_7\Omega_1 + k_8\Omega_2 \tag{5}$$

being λ, ϖ and Ω the mean longitudes, longitudes of the perihelia and longitudes of the nodes respectively, k_0, k_1, k_2 are integers fixed by the resonance and the $k_{i>2}$ are arbitrary integers but verifying the d'Alembert condition

$$\sum_{i=0}^{8} k_i = 0 \tag{6}$$

$\mathcal{P}_j$ is a polynomial function depending on the eccentricities and inclinations which its lowest order term is

$$C e_0^{|k_3|} e_1^{|k_4|} e_2^{|k_5|} \sin(i_0)^{|k_6|} \sin(i_1)^{|k_7|} \sin(i_2)^{|k_8|} \tag{7}$$

The calculation of the coefficients C is a very laborious task that must be done case by case and it is so challenging that only the planar case was studied by analytical methods and consequently there are not expansions involving $\sin(i_i)$ published up to now. An example of this development can be found in Gomes (2012) where an expansion for a specific 3BR in an extrasolar planar system is obtained. The expansion given by Eq. (3) implies that for a given resonance there are several σ_j contributing to the resonant motion. Each σ_j generates specific dynamical effects and the joint action of all σ_j is called multiplet. Nevertheless, the expansion (3) can be reduced to a few terms when the eccentricities and inclinations are very small. In particular, when $e_1 = e_2 = i_1 = i_2 = 0$ the lowest order non null terms for $\mathcal{P}_j$ are those with $k_4 = k_5 = k_7 = k_8 = 0$:

$$C e_0^{|k_3|} \sin(i_0)^{|k_6|} \cos(k_0\lambda_0 + k_1\lambda_1 + k_2\lambda_2 + k_3\varpi_0 + k_6\Omega_0) \tag{8}$$

from which can be deduced that for three coplanar orbits ($i_0 = 0$) the only non null terms are those with $k_6 = 0$, and consequently the lowest order term in the expansion is proportional to e_0^q, where $q = |k_3|$. This explain why the lower the order the stronger the resonance. In case that $e_0 = 0$ but with $i_0 \neq 0$ the non null terms are those with $k_3 = 0$ which result proportional to $\sin(i_0)^q$ instead, where $q = |k_6|$. But, as we explain below, if $|k_6|$ is odd the resulting principal term of the expansion is proportional to $\sin(i_0)^{2q}$. Note that for coplanar circular orbits all terms are null except for zero order resonances because in this special case the principal terms are independent of e_i, i_i.

To avoid the difficulties of the analytical methods Gallardo (2014) proposed a semianalytical method for the estimation of the strength of a resonance on a massless particle in an arbitrary orbit under the effect of two perturbing planets in circular coplanar orbits. The method, which is essentially an estimation of the amplitude of the disturbing function factorized by an arbitrary constant coefficient, was applied to minor bodies captured in 3BRs with the planets of the Solar System. In the present work, in Section 2 we extend the method to a system of three massive bodies with arbitrary orbits and we apply it to an hypothetical planetary system in order to analyze the dependence of the strengths on the orbital parameters. In Section 3 we explore by numerical methods some of the properties of the resonances that our method predicts and we apply the method to the case of the Galilean satellites. The conclusions are presented in Section 4.

2. Strength for planetary three body resonances and its dependence with the parameters

Strictly, 3BRs between three planets P_0, P_1 and P_2 with elements (a_i, e_i, i_i, Ω_i, ϖ_i) and masses m_0, m_1 and m_2 around a star of mass M occur when a particular critical angle given by Eq. (4) is oscillating over time. In this work we call $p = |k_0| + |k_1| + |k_2|$ and we note as $k_0 + k_1 + k_2$ the resonance involving the three planets, where always $k_0 > 0$. We will not consider the case of 3BRs as result of superposition of 2BRs because the 2BRs will override the dynamical effects of the 3BR we are trying to study, with the exception of systems with near zero eccentricity orbits. We will consider the planets P_1 and P_2 at fixed semimajor axes $a_1 < a_2$ and the third "test" planet P_0 with the semimajor axis defined by the resonant condition which can result in an internal, external o middle position with respect to P_1 and P_2. The approximate nominal location of the test planet P_0 assumed in the resonance $k_0 + k_1 + k_2$ is deduced from Eq. (1):

$$a_0^{-3/2} \simeq -\frac{k_1\sqrt{(M+m_1)}}{k_0\sqrt{(M+m_0)}} a_1^{-3/2} - \frac{k_2\sqrt{(M+m_2)}}{k_0\sqrt{(M+m_0)}} a_2^{-3/2} \tag{9}$$

which must be positive otherwise the resonance does not exist. In order to obtain a numerical estimation of the resonance's strength we extended the method given by Gallardo (2014) to a system of three massive bodies with arbitrary orbits. The details of the method and the devised algorithm can be found in the Appendix. Essentially, this new method predicts different strengths called S_0, S_1, S_2 for the three massive bodies, that means, each massive body feels the resonance in a different way. Each S is related to the amplitude of the variations of $\mathcal{R}$ in Eq. (3) caused by the cumulative effect of all involved terms. Then, the method cannot distinguish between the dynamical effects of each term of a multiplet for a given resonance, it only provides a global estimation.

In order to test the algorithm and to explore the dependence of the strengths with the different parameters involved we applied it to an hypothetical planetary system with $m_1 = m_2 = 0.0001 M_\odot$, $a_1 = 1.0$ au, $a_2 = 3.6$ au around a star with 1 $M_\odot$ and we calculate all resonances with $q \leq 9$ and $p \leq 30$ between 2.0 au and 2.6 au, that means with the planet P_0 located in between and excluding close-encounter situations. With the exception of Section 3.3,

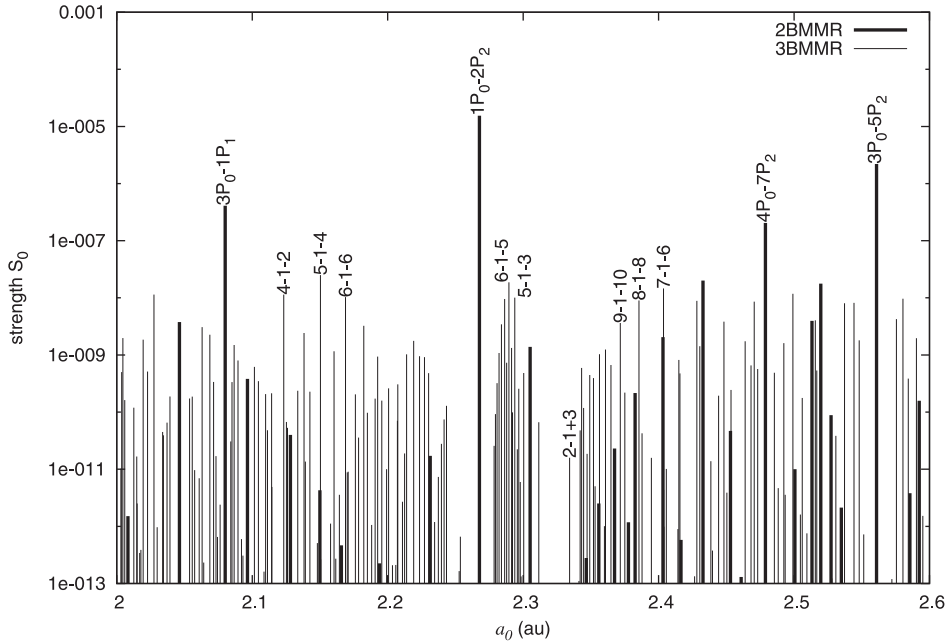

Fig. 1. Location and strength of the main 3BRs (thin lines) and location and relative strengths of the 2BRs (thick lines) for the hypothetical working system with a planet P_1 at 1 au and planet P_2 at 3.6 au. The horizontal axis corresponds to the value of the semimajor axis a_0 of the test planet P_0 and the vertical axis corresponds to the strengths of the possible 3BRs. The strengths were calculated assuming $e_i = 0.05$, $i_i = 1.0$ degree, $m_i = 0.0001$ and the other elements taken from Table 1. Some two body and three body resonances are labeled. The 2BRs were plotted in a different scale than the 3BRs and they are indicated only for reference.

Table 1
Working example of an hypothetical planetary system with the range of variation of the orbital elements assumed in the calculations. The mass of the central star is 1 $M_\odot$.

Body	a (au)	e	i(°)	Ω(°)	ϖ(°)	m ($M_\odot$)
P_0	(2, 2.6)	(0, 0.3)	(0, 10)	0	60	(0, 0.01)
P_1	1.0	(0, 0.1)	(0, 10)	120	180	1×10^{-4}
P_2	3.6	(0, 0.1)	(0, 10)	240	300	1×10^{-4}

in the examples presented along this paper P_0 is located between the other two planets, but our method is valid for arbitrary positions of P_0 with respect to P_1 and P_2. The complete set of orbital parameters with their variation range used in our experiments can be found in Table 1. Fig. 1 shows the main resonances in the interval where the strength of the 2BRs involving P_0 with planets P_1 or P_2 were calculated following the algorithm proposed in Gallardo (2006) and the 3BRs were calculated with the algorithm proposed here. The set of 2BRs is not in the same scale of the set of 3BRs because they have different definitions. All codes can be downloaded from www.fisica.edu.uy/~gallardo/atlas.

2.1. Effect of varying m_0 and the restricted case, $m_0 = 0$

To test the effect of the planetary mass on the strengths we choose the zero order resonance $6-1-5$ located at $a = 2.2894$ au and calculate the three strengths S_0, S_1, S_2 varying m_0. The results presented in Fig. 2 show that when m_0 tends to zero S_0 is unaffected but S_1, S_2 tend to zero, that means the 3BR over P_0 survive because is proportional to $m_1 m_2$ but the other two planets tend to loose the resonance because their respective strengths are factorized by m_0. This behavior is similar for all resonances independently of the order. For growing m_0, S_0 is unaffected but S_1, S_2 grow proportionally to m_0 and when m_0 is equal to the other masses, S_0 nevertheless is greater than S_1 and S_2. In general, for similar masses the planet in the middle is the one with the greater dynamical effect, which is in agreement with results obtained by Quillen (2011) for zero order resonances. The fact that S_0 is independent of m_0 is not evident from Eqs. (A.5)–(A.26) but it is an evident result from the analytical theories of 3BRs, see for example Ferraz-Mello (1979) or Quillen (2011). This concordance between numerical and analytical results gives support to our proposed algorithm, at least with respect to the role of the involved masses.

When considering the restricted case, $m_0 \to 0$, with P_1 and P_2 in circular and coplanar orbits it is easy to show that we reproduce the results of the restricted case obtained by Gallardo (2014). That means $S_1 \sim S_2 \sim 0$ and it is clear a strong dependence of S_0 on the order q. For coplanar orbits $S_0 \propto e_0^q$ and for zero eccentricity orbits $S_0 \propto \sin(i_0)^q$ for even q and $S_0 \propto \sin(i_0)^{2q}$ for odd q as in Gallardo (2014). This dependence on inclination is understood because by d'Alembert rules the inclinations only appear with even exponents in the development of the disturbing function. For $e_0 = 0$ the lowest order term is proportional to

$$\sin(i_0)^{|k_6|} \cos(k_0\lambda_0 + k_1\lambda_1 + k_2\lambda_2 + k_6\Omega_0) \tag{10}$$

and due to Eq. (6) we have $|k_6| = |k_0 + k_1 + k_2| = q$, being k_6 even. Then, if q is odd the lowest order non null term is the next harmonic, which is

$$\sin(i_0)^{|2k_6|} \cos(2k_0\lambda_0 + 2k_1\lambda_1 + 2k_2\lambda_2 + 2k_6\Omega_0) \tag{11}$$

and then $S_0 \propto \sin(i_0)^{2q}$.

Now, we can apply the present method to the case of excited orbits for P_1 and P_2, not considered in Gallardo (2014). In this case we obtain that the dependence with q is not so clearly defined as in the case with circular planar orbits for P_1 and P_2 showed in Gallardo (2014). We can explain this result looking at the relevant terms of the disturbing function. For the coplanar case with $e_1 = e_2 = 0$ the only relevant term is the one factorized by e_0^q. But, for non circular orbits several terms factorized by $e_0^l e_1^m e_2^n$, with l, m, n integers, contribute to the disturbing function and, if there is some mutual inclination, terms depending on the inclinations will also appear. We will show this behavior below for the non restricted case ($m_0 > 0$).

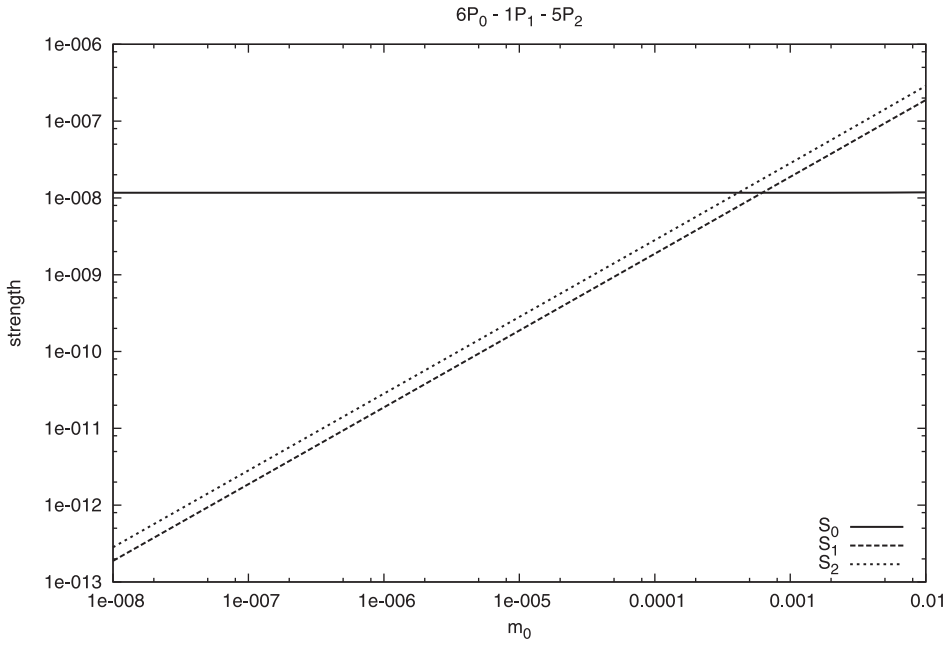

Fig. 2. Strengths as function of m_0 for resonance $6-1-5$. The three planets are assumed with $e_i = 0.1$ and $i_i = 0$. The planet having its mass varying is not affected by its own mass (S_0 is constant) but the other two planets have strengths proportional to m_0. When the three masses are equal the greater strength is S_0, that means the planet in the middle.

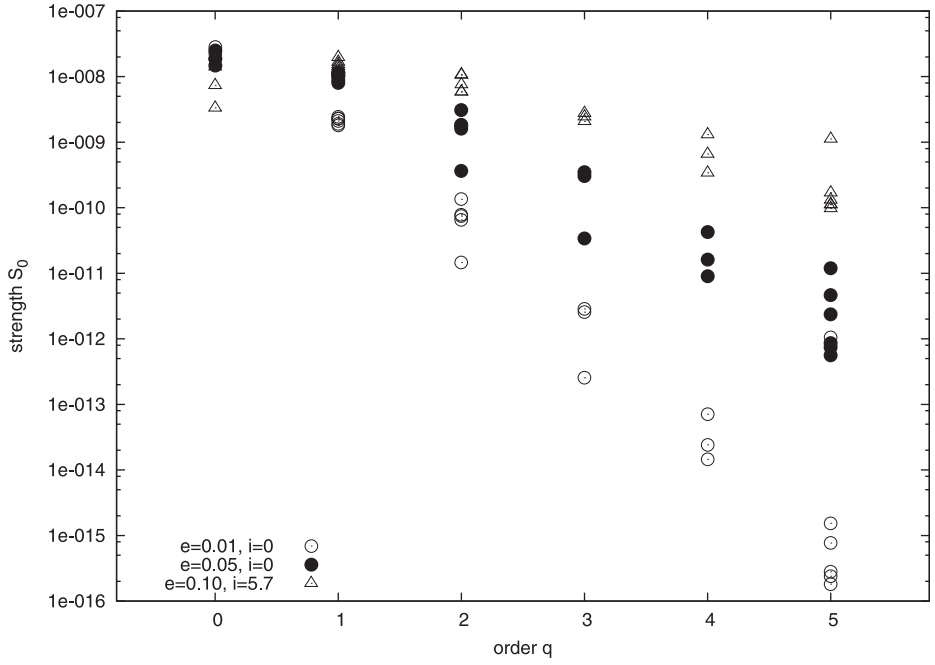

Fig. 3. Strengths for planet P_0 of the lowest order 3BRs from Fig. 1. Strengths were calculated for three different orbital states: coplanar and near zero eccentricities (open circles), coplanar and low-excited eccentricities (filled circles) and dynamically excited orbits (triangles). The greater the dynamical excitation the lesser the dependence with the order q.

2.2. Dependence with the resonance order q

Fig. 3 shows the strengths for planet P_0 assumed to be located in each of all resonances between 2.0 and 2.6 au with $p < 15$ and $q \leq 5$ for three different orbital configurations for the three planets: coplanar and almost circular orbits, coplanar and Jupiter-like eccentricity orbits and dynamically excited orbits ($e = \sin(i) = 0.1$). The dependence with the order is strong for near zero eccentricities in contrast with the excited orbits where high order resonances are as important as the zero order. Then, for near coplanar and circular orbits only zero order resonances are dynamically relevant, but for excited orbital configurations high order resonances can also be dynamically relevant, a not surprising fact that it is well known for the case of 2BRs. Fig. 3 refers to the strength S_0 over planet P_0 located in between but we have also analyzed the strength S_1 over the innermost planet and S_2 over the exterior planet. In Fig. 4 we show the three S_i for each resonance where we obtained systematically $S_1 < S_0$, that means, the inner planet experiences less dynamical effects than the planet in the middle. For $q \leq 1$ we obtained also $S_2 < S_0$ in agreement with Quillen (2011), but for $q \geq 2$ the rule is not always verified.

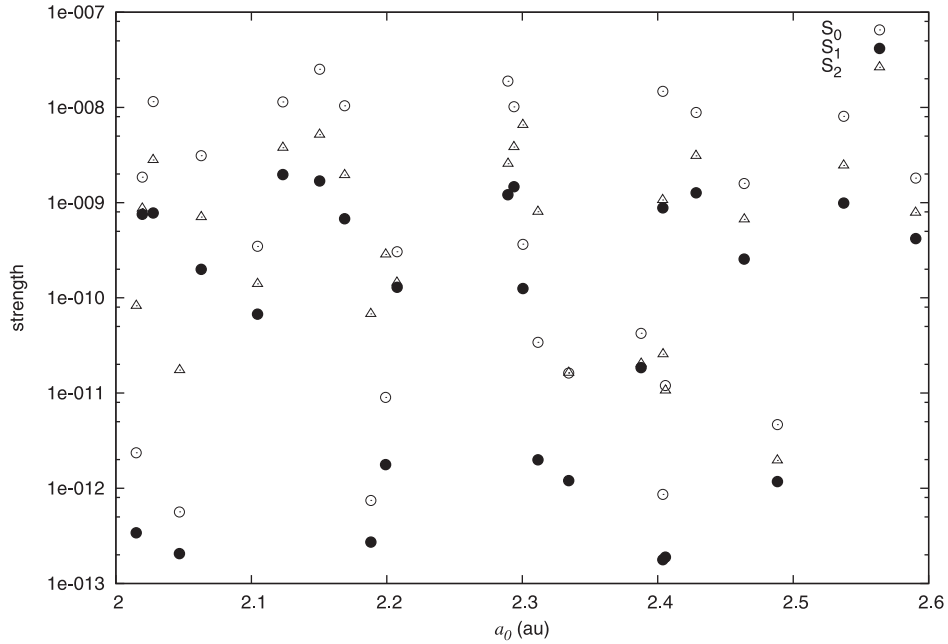

Fig. 4. Strengths for the three planets for some 3BRs from Fig. 3 calculated for coplanar orbits with $e = 0.05$. For each resonance defined by a_0 the strengths for each planet are showed. In general it is verified $S_1 < S_2 < S_0$.

2.3. Dependence with eccentricity

Fig. 5 shows the strengths as function of e_0 for the four order resonance $2-1+3$ located at 2.3343 au taking coplanar planets with $e_1 = e_2 = 0$ in one case and with $e_1 = e_2 = 0.1$ in other case. In the first case the strengths S_0, S_1 and S_2 are proportional to e_0^q being $q = 4$ as expected for a four order resonance. For the second case, when the planets are in eccentric orbits, the dependence with e_0 is not so clear mathematically. The reason is that when the perturbing planets are eccentric there is not a unique term governing the disturbing function as we have already explained, see for example Nesvorný and Morbidelli (1999) and Gomes (2012). This behavior for circular and excited orbits is similar for all non zero order resonances.

2.4. Dependence with inclination

One of the advantages of the semianalytical method is that we can easily explore the dependence of the resonances strengths with orbital inclinations. Fig. 6 shows the strengths as function of i_0 for the first order resonance $5-1-3$ located at 2.2939 au taking circular orbits with $i_1 = i_2 = 0^\circ$ in one case and with $i_1 = i_2 = 5.7^\circ$ in other case. In the first case, the strengths depend on $(\sin i)^{2q}$ as expected for an odd-order resonance as we have explained above. In analogy to the case of a planetary system with excited orbits, the circular but inclined cases show resonance strengths with a not so well defined dependence with i_0 due to the several relevant terms in the disturbing function. This figure is probably the first one published showing the effect of the orbital inclination on a planetary 3BR.

2.5. Zero order resonances

Fig. 7 shows the strengths as function of e_0 for the zero order resonance $6-1-5$ located at 2.2895 au. They are almost independent of the eccentricity in the range $0 < e_0 < 0.1$. Fig. 8 shows the strengths as function of i_0 and in analogy to the previous figure we can check they are almost independent of the inclinations in the range $0 < \sin(i_0) < 0.1$. Zero order resonances exhibit this property of being almost independent of e and i, at least in the range of low eccentricity and low inclination orbits.

For zero order resonances we can compare our results with the theory by Quillen (2011) for closely spaced planetary systems. For example we calculated the strengths for the hypothetical system composed by $a_1 = 1$ au, $a_0 = 1.1586$ au and $a_2 = 1.4$ au which a_0 corresponds to the resonance $2-1-1$ assuming coplanar and circular orbits. With our algorithm we obtained $S_2/S_1 = 1.3$ and $S_0/S_1 = 3.8$ while using formulae (29) by Quillen (2011) we obtain $\Delta a_2/\Delta a_1 = 1.2$ and $\Delta a_0/\Delta a_1 = 2.1$, results in reasonable agreement taking into account the very different approaches involved and that in principle there is not necessarily a linear relation between strength and Δa.

2.6. Conclusions about the algorithm

The algorithm presented in the Appendix provides reasonable estimates of the resonances strengths on each of the three massive bodies involved in a 3BR. Also, the behavior of the functions S are coherent with known analytical results. In particular, the behavior of the strengths with the masses, orbital elements and order of the resonances is in agreement with that we can expect from the analytical expression of the disturbing function. The examples presented above show that the resonance strength for a given planet is proportional to the masses of the two other planets as expected; thus the planet with the lowest mass is the one most affected by the resonance but for comparable masses the planet in the middle is in general the one that suffers the greatest dynamical effects. For low eccentricity and inclination orbits there is a neat dependence of the strengths with e, i and the order. For a system with excited orbits in (e, i), the dependence of the strengths with (e, i) is not so clear mathematically and almost constant in the range (0,0.1) in e and $\sin i$. For planetary or satellite systems with near circular near coplanar orbits only zero order resonances are dynamically relevant but for excited systems, resonances of higher order may also be dynamically relevant.

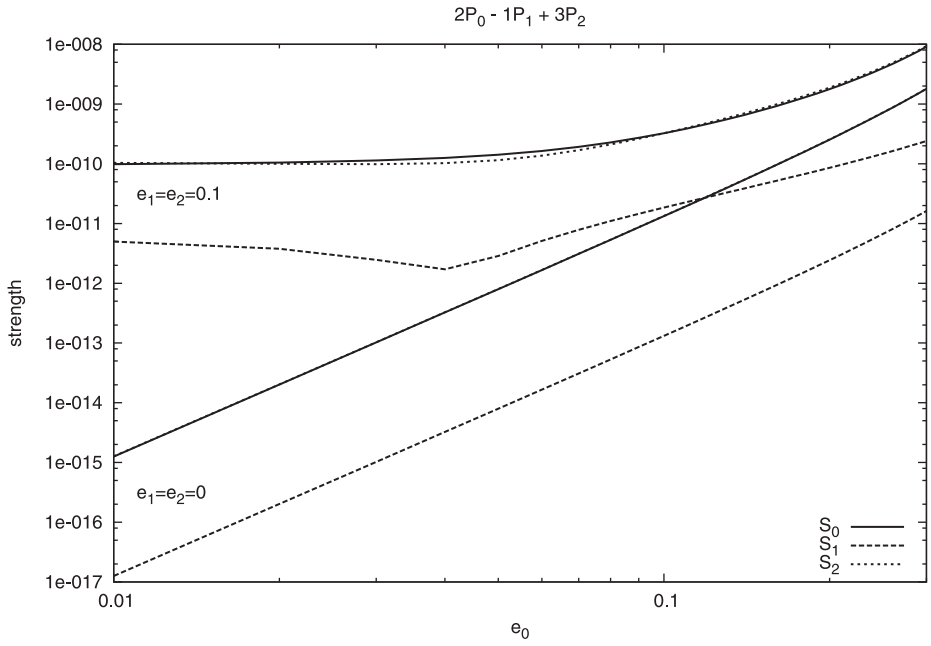

Fig. 5. Strengths S_0, S_1, S_2 for the three planets in coplanar orbits as function of e_0 for the four order resonance $2-1+3$. Two cases are showed: $e_1 = e_2 = 0$ in lower curves and the excited case $e_1 = e_2 = 0.1$ in upper curves. The dependence of S_i with e_0 is mathematically very clear in the first case ($S_i \propto e_0^4$) but not in the excited one. S_0 and S_2 are almost equal in this resonance.

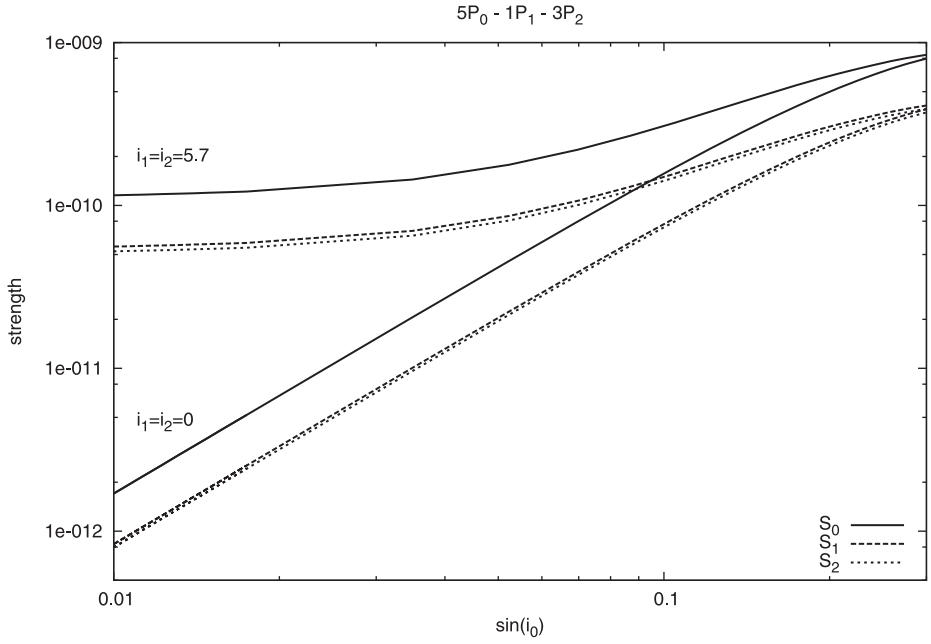

Fig. 6. Strengths S_0, S_1, S_2 for the three planets assumed in circular orbits as function of i_0 for the first order resonance $5-1-3$. Two cases are showed: $i_1 = i_2 = 0$ in lower curves and the inclined case $i_1 = i_2 = 5.7$ in upper curves. In analogy with Fig. 5, the dependence of S_i with i_0 is mathematically very clear in the first case ($S_i \propto \sin(i_0)^2$) but not in the second one.

3. Numerical experiments

In this section we explore the dynamical properties of some 3BRs by means of numerical methods and we compare the results with the predictions of our algorithm. The numerical integrations were carried out with adaptations of the code EVORB (Fernández et al., 2002).

3.1. Defining domains in a,e,i with dynamical maps

We implemented codes in FORTRAN to construct dynamical maps near some 3BRs. In particular, from Fig. 1 we choose the resonance $5-1-4$ near $a \simeq 2.15$ au. The dynamical maps in (a, e) were constructed taking a grid of $\simeq$ 10000 initial conditions for P_0 and calculating the time evolution of its semimajor axis over a small number of libration periods, which it is about 15000 years. We calculate the mean $\bar{a}$ over a period of 1000 years in order to remove short period oscillations and moving this window over the entire integration we obtain $\bar{a}(t)$, which approximately represents the time evolution of the semimajor axis due to the resonance's dynamical effects. Then, we calculate the amplitude $\Delta\bar{a} = \bar{a}_{max} - \bar{a}_{min}$ and plot this value as function of the initial (a, e) with a gray scale from white to black according to increasing values of $\Delta\bar{a}$. The structures that appear in Fig. 9 are due to

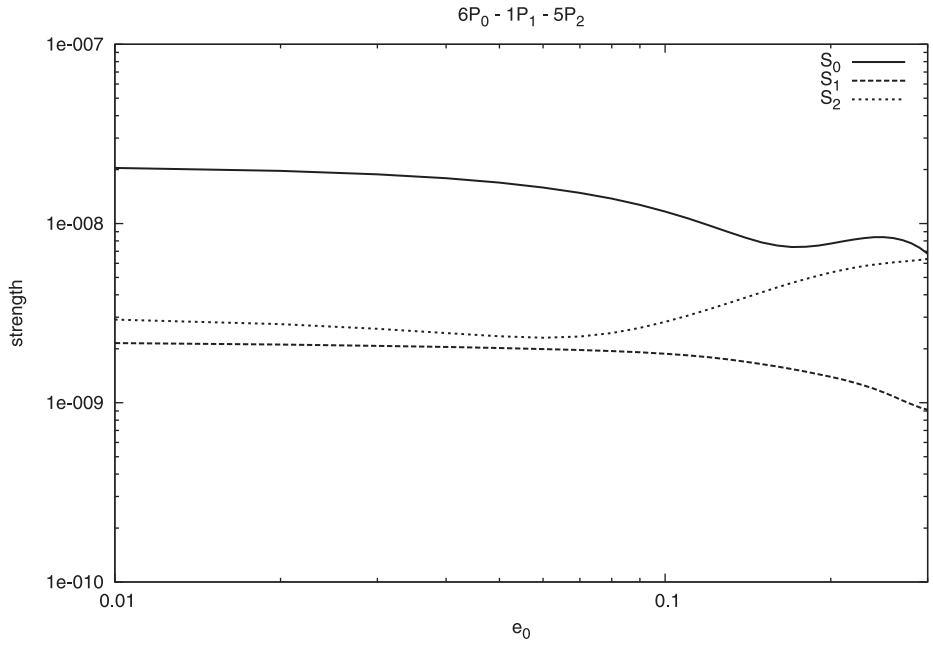

Fig. 7. Strengths as function of e_0 for the zero order 3BR $6-1-5$. All other eccentricities are equal to 0.1 and all inclinations are zero. For small eccentricities, the strength for each planet is almost independent of the eccentricity, as is typical for zero order resonances.

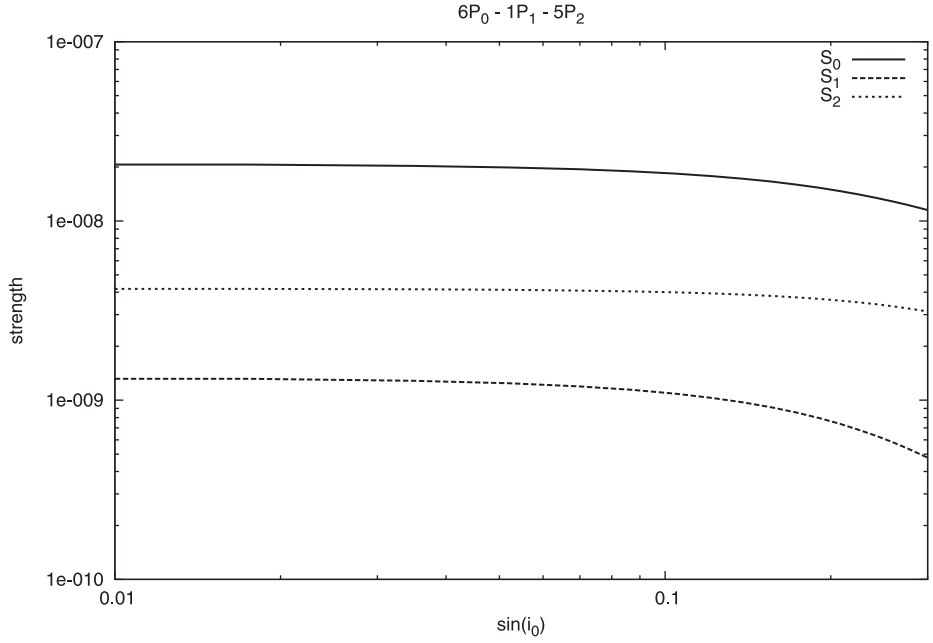

Fig. 8. Strengths as function of i_0 for the same 3BR of Fig. 7. All are circular orbits. All other inclinations are equal to 5.7°. The strength for each planet is almost independent of the inclination as is typical for zero order resonances.

the dynamical effects of two resonances: the one at the right is due to the 3BR $5-1-4$ and the one at the left is due to the high order 2BR $6P_0-13P_2$. Each one shows a central region due to small amplitude oscillations, a dark border region with large amplitude oscillations near the separatrix and an exterior region outside the resonance with near zero amplitude oscillations typical of a secular evolution. To identify these resonances we implemented another code that calculates the corresponding critical angles during the same time interval of the numerical integration and performs a statistical analysis comparing the computed values of the critical angle with a uniform distribution between 0 and 360 degrees. Large departures from the uniform distribution, meaning small amplitude librations, are represented with black pixels and small departures, meaning large amplitude or circulations, are represented with white pixels. The resulting map for the critical angle $\sigma=5\lambda_0-\lambda_1-4\lambda_2$ is showed in Fig. 10 and the map for $\sigma=6\lambda_0-13\lambda_2+7\varpi_0$ is showed in Fig. 11 which confirm that the dynamical effects showed in Fig. 9 are due to these resonances. It is interesting to note that at small eccentricities both critical angles librate but, looking at Fig. 9, we can verify that the high order 2BR have null dynamical effects meanwhile the zero order 3BR have appreciable effects in semimajor axis even at zero eccentricities, which is in agreement with the theory and the predictions of our semianalytical method. At near zero eccentricities the dynamically relevant resonances are only those of order zero.

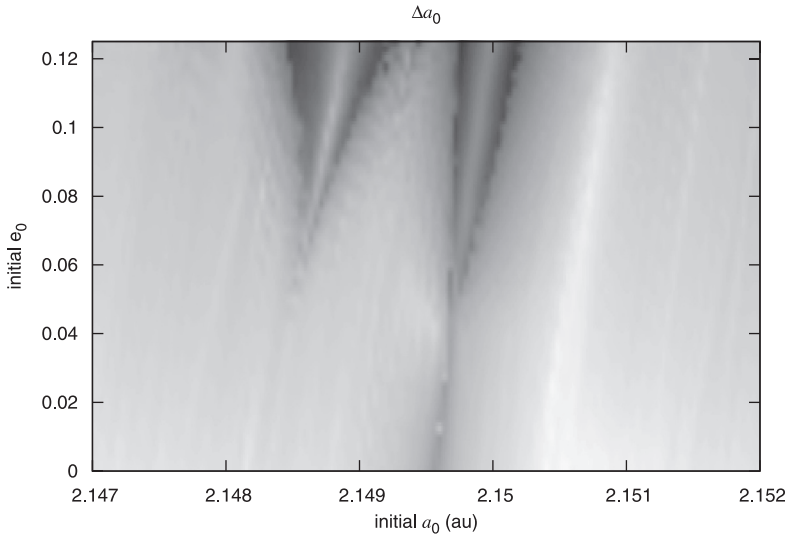

Fig. 9. Dynamical map showing the domains of the resonances in (a_0, e_0) for $e_1 = e_2 = 0.01$, $i_i = 1^\circ$ and $m_i = 0.0001 M_\odot$. At the left is the 2BR $6P_0 - 13P_2$ and at right the 3BR $5 - 1 - 4$. Dark regions correspond to large amplitude (10^{-4} au) oscillations of $\bar{a}_0$ and light regions to small amplitude (10^{-7} au) oscillations. When varying m_0 this map remains unchanged. On the other hand, when increasing m_1 the 3BR increases its domain while the 2BR remains unchanged.

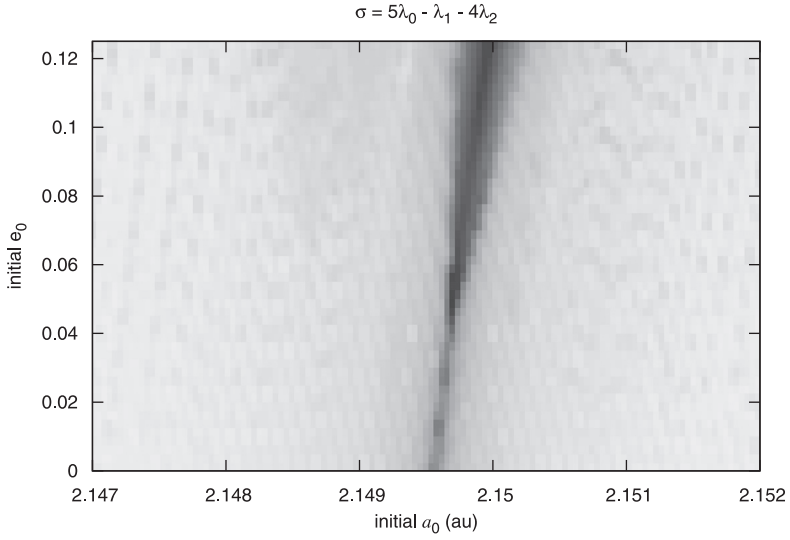

Fig. 10. Behavior of the critical angle $\sigma = 5\lambda_0 - \lambda_1 - 4\lambda_2$ corresponding to the 3BR for the same domain of Fig. 9. Black regions correspond to librations and they match very well with the domain of the 3BR showed in Fig. 9.

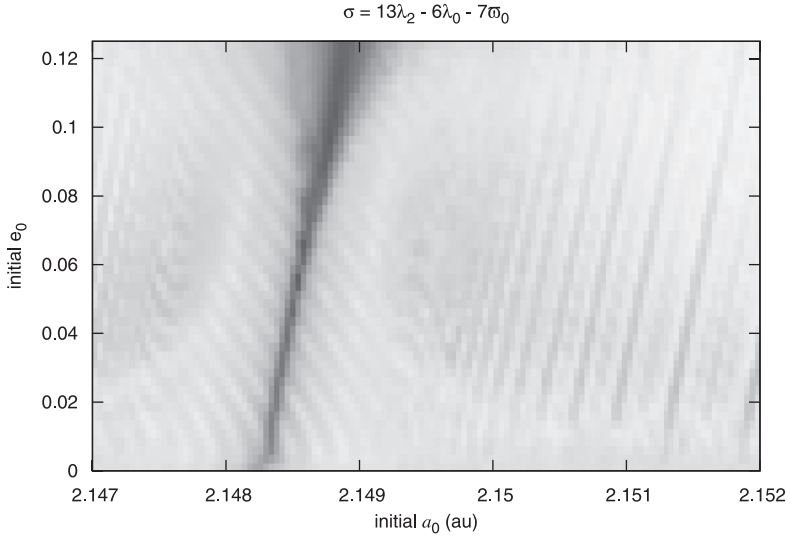

Fig. 11. Behavior of the critical angle $\sigma = 6\lambda_0 - 13\lambda_2 + 7\varpi_0$ corresponding to the 2BR for the same domain of Fig. 9. Black regions correspond to librations and they match very well with the domain of the 2BR showed in Fig. 9.

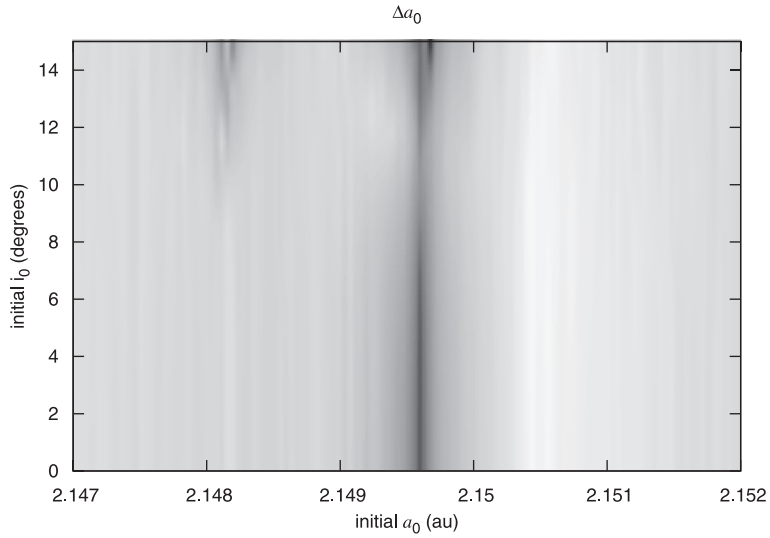

Fig. 12. Dynamical map showing the domains of the resonances in (a_0, i_0) for $e_i = 0.01$, $i_1 = i_2 = 0.1^\circ$. Dark regions correspond to large amplitude (10^{-5} au) oscillations of $\bar{a}_0$ and light regions to small amplitude (10^{-7} au) oscillations. The domain of the 3BR is unaffected by i_0 while the 2BR shows up only for large inclinations.

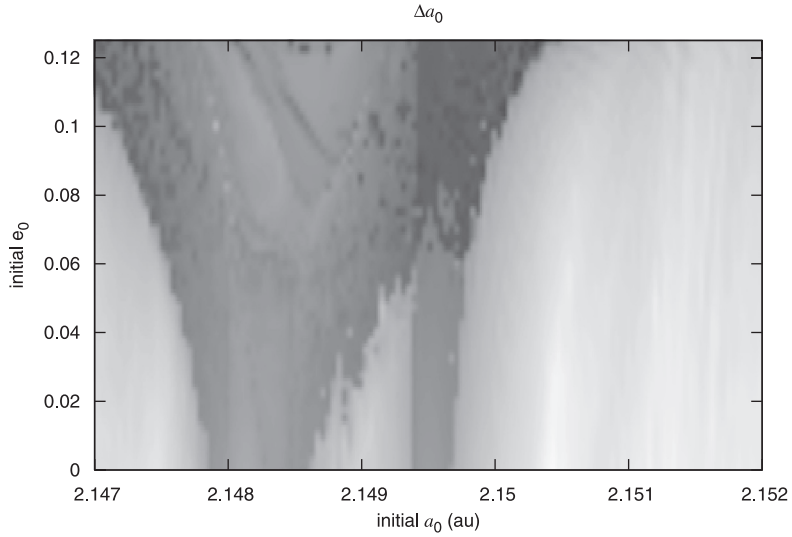

Fig. 13. Same as Fig. 9 but for an excited system with $e_1 = e_2 = 0.1$, $i_i = 10^\circ$. Dark regions correspond to large amplitude (10^{-3} au) oscillations of $\bar{a}_0$ and light regions to small amplitude (10^{-7} au) oscillations. The 2BR has grown by a very large amount erasing the traces of the 3BR for $e_0 > 0.06$.

The resonance domain in (a, i) is represented in the map given in Fig. 12 which was calculated taking $e_i = 0.01$ and $i_1 = i_2 = 0.1^\circ$. Both resonances can be distinguished and as we have remarked previously the domain of the zero order 3BR is almost independent of the inclination while the high order 2BR is strongly dependent on inclination being vanishingly small at low inclinations.

The last map presented in Fig. 13 was generated for a dynamically excited system and shows an impressive growth of the 2BR that overrides the 3BR for $e_0 > 0.05$ illustrating that for excited systems 2BRs must dominate over the 3BRs. Note also that the domain of the 3BR is almost independent of the eccentricity. Nevertheless, back to Fig. 9, it is supposed that a zero order 3BR must be almost independent of the eccentricity while it is showed some growing of its domain for $e_0 > 0.06$ not only in Fig. 9 but also in Fig. 10. This seems contradictory with our results for zero order 3BRs. We have checked that there are not 2BRs superposed to the 3BR, then we can conjecture that the multiplet of this resonance generate that feature. The multiplet is composed by a principal term independent of e plus several terms depending on powers of the eccentricity.

3.2. Libration properties and dynamical evolution in a migrating scenario

Libert and Tsiganis (2011) studied the capture of a system in a chain of 2BRs due to a migration scenario. For the initial conditions they considered, they found that, as a general rule, the two inner planets are captured in a 1:2 resonance and the third planet is captured in the 1:2 or 1:3 resonance with the middle one. This configuration allows a very interesting evolution in eccentricity and inclination and the resulting 3BR is in fact a superposition of 2BRs. In particular the semimajor axes evolve as expected for two planets locked in a 2BR maintaining a constant ratio as they evolve towards the star due to the migration mechanism. In this paper we are interested in detecting dynamical mechanisms generated by pure 3BRs, that means not reducible to a superposition of 2BRs which, in general, are stronger and then they could erase the effects of the 3BRs.

A dynamical evolution of a pure 3BR is exemplified in Fig. 14 where we show the time evolution of the mean a_i together with the time evolution of the critical angle

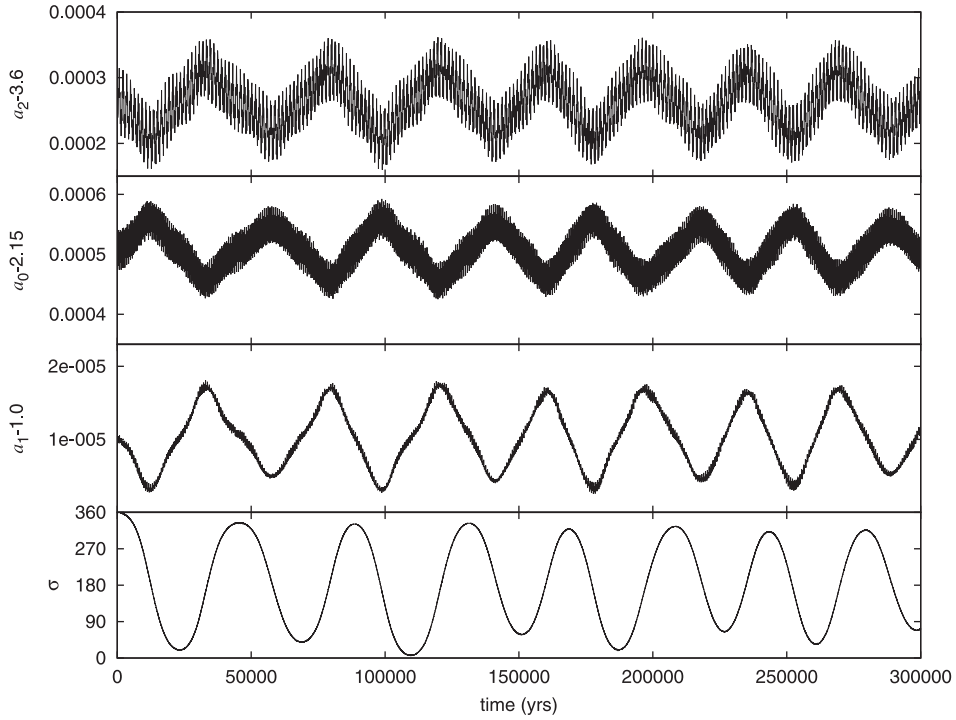

Fig. 14. Time evolution of a planetary system inside the zero order pure 3BR $5-1-4$ with P_1 and P_2 at the same positions of the previous figures. Initial values are $e_i = 0.01$ and $i_i = 1^\circ$. The mean semimajor axes were calculated with a moving window of 500 years. The critical angle is $\sigma = 5\lambda_0 - \lambda_1 - 4\lambda_2$. The oscillations of the planet in the middle are opposed to the oscillations of the other two planets.

$\sigma = 5\lambda_0 - \lambda_1 - 4\lambda_2$ for the same working planetary system we have idealized in Fig. 1 with initial conditions near the border of this zero order 3BR. Mean a_i were calculated with a running window of 500 years. The time evolution of the semimajor axes are in agreement with the theoretical results by Quillen (2011) who showed that, at least for zero order 3BRs, the exterior and interior planet have semimajor axes oscillating in phase and the planet in the middle is half period shifted. Also, running our algorithm for this case we obtain $S_0/S_1 \simeq 13$ and $S_0/S_2 \simeq 4$ which can be compared with the Δa taken from Fig. 14: $\Delta a_0/\Delta a_1 \sim 10$ and $\Delta a_0/\Delta a_2 \sim 1$. It is not an exact match because S_i probably is not directly proportional to Δa_i, but we can conclude our strengths S_i are coherent with the dynamical effects observed in the semimajor axes of the involved bodies.

In the next numerical experiment we simulate a migration of the exterior planet P_2 towards the central star while the system evolves inside the first order 3BR $4-1-2$. The migration of the outer planet P_2 is imposed by an artificial constant force with direction contrary to the orbital velocity generating a variation rate of $\dot{a} = -1 \times 10^{-8}$ au/yr. The resulting evolution is showed in Fig. 15 where undoubtedly the three semimajor axes evolve in synchrony with the oscillations of the critical angle and is again verified that the oscillations of the semimajor axes of the exterior and interior planets are in phase while the planet in the middle is shifted half a period. Also, a not very intuitive phenomena is observed: while the outer two planets migrate inwards the inner planet P_1 migrates outwards. Contrary to the case of systems captured in a 2BR where, in general, both semimajor axes must grow or decrease simultaneously linked by the resonant relation, in the case of 3BRs there is another degree of freedom that allows this behavior. Nevertheless, it is important to mention that for planetary systems with very low eccentricity orbits trapped in 2BRs it is possible to observe divergence of orbits as showed by Batygin and Morbidelli (2013) because for low eccentricity orbits the location of the resonance is shifted in semimajor axes due to the Law of Structure of the resonance (Ferraz-Mello, 1988) which is a dependence of a_{res} on the orbital eccentricity. Then, if the eccentricities change, being small, the ratio a_1/a_2 of a pair of planets locked in resonance can change due to the Law of Structure. We have simulated other migrations processes with systems inside other pure 3BRs and we have obtained that is very common that the planets migrate with diverging orbits not only for low eccentricity orbits but also for excited orbits.

We performed a series of numerical experiments trying to capture a planetary system in a 3BR from outside the resonance in a migrating scenario using migration rates from 10^{-9} to 10^{-6} au/yr both positive and negative. Our very preliminary results indicate that capture in a pure 3BR is a very rare event while capture in a chain of 2BRs is a very frequent result as has been demonstrated by Libert and Tsiganis (2011). An example of this last case is showed in Fig. 16 where an external migrating planet P_2 with $\dot{a} = -1 \times 10^{-6}$ au/yr captures the middle planet P_0 in the $3P_0 - 5P_2$ resonance at $t = 42000$ years and then P_0 captures the planet P_1 in the resonance $9P_0 - 5P_1$ at $t = 111000$ years. Consequently the system gets trapped in the zero order 3BR $3-1-2$ which is the lowest order 3BR that can be obtained from the two 2BRs, but its dynamics is mostly due to the superposition of the mutual 2BRs. In this example all three planets have $m = 10M_\oplus$, initial $e_i = 0.01$ and mutual inclinations of about 1 degree. Our experiments show systematically that when the system cross a 3BR the three planets experience a jump in semimajor axes: the planets in the extremes have a jump in the same direction and the planet in the middle in the contrary direction, in agreement with Quillen (2011). The capture in pure 3BRs deserves much more study and is beyond the scope of this work.

3.3. Application to the Galilean satellites

We applied our semi-analytical method to explore all possible 3BRs between Galilean satellites near the location of Europa.

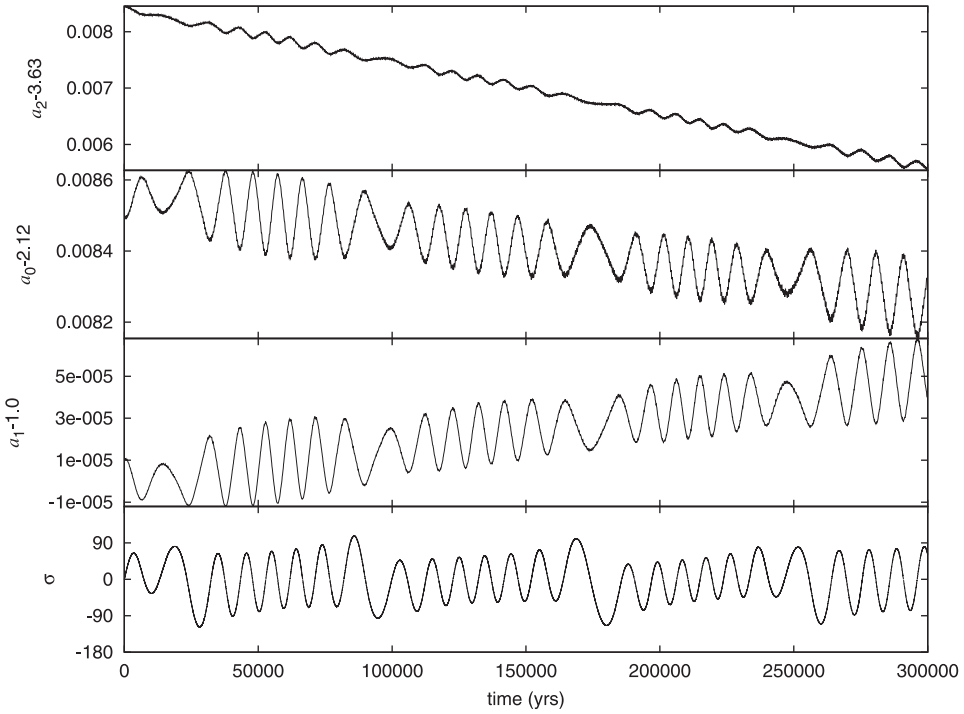

Fig. 15. Time evolution of a planetary system inside the pure first order 3BR $4-1-2$ imposing a forced inward migration for P_2. Initial values are $e_i = 0.01$ and $i_i = 1^\circ$. Mean semimajor axes calculated with a moving window of 500 years. The critical angle is $\sigma = 4\lambda_0 - \lambda_1 - 2\lambda_2 - \varpi_1$. A system inside a 3BR when forced to migrate can exhibit rate changes positive and negative for the semimajor axes.

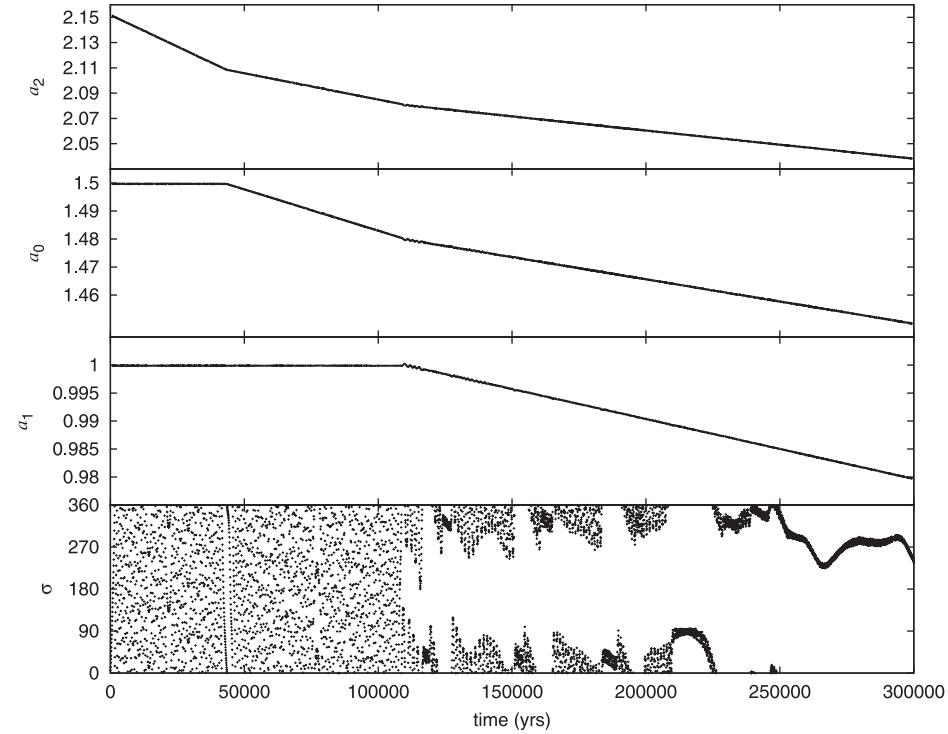

Fig. 16. Capture and evolution in a chain of two 2BRs imposing a forced inwards migration of P_2. The critical angle showed at bottom is $\sigma = 3\lambda_0 - \lambda_1 - 2\lambda_2$. Mean semimajor axes calculated with a moving window of 1000 years. A system captured in a chain of 2BRs when forced to migrate in general exhibit rate changes of the same sign for the semimajor axes.

Table 2
Mean orbital elements for Epoch 1997 Jan. 16.00 TT taken from ssd.jpl.nasa.gov. $J_2 = 14.7 \times 10^{-3}$.

Satellite	a (au)	e	i(°)	Ω(°)	ω(°)	M(°)	m ($M_\odot$)
Io	0.002812	0.0041	0.036	43.977	84.129	342.021	4.5D-08
Europa	0.004474	0.0094	0.466	219.106	88.970	171.016	2.4D-08
Ganymede	0.007136	0.0013	0.177	63.552	192.417	317.540	7.6D-08
Callisto	0.012551	0.0074	0.192	298.848	52.643	181.408	5.4D-08

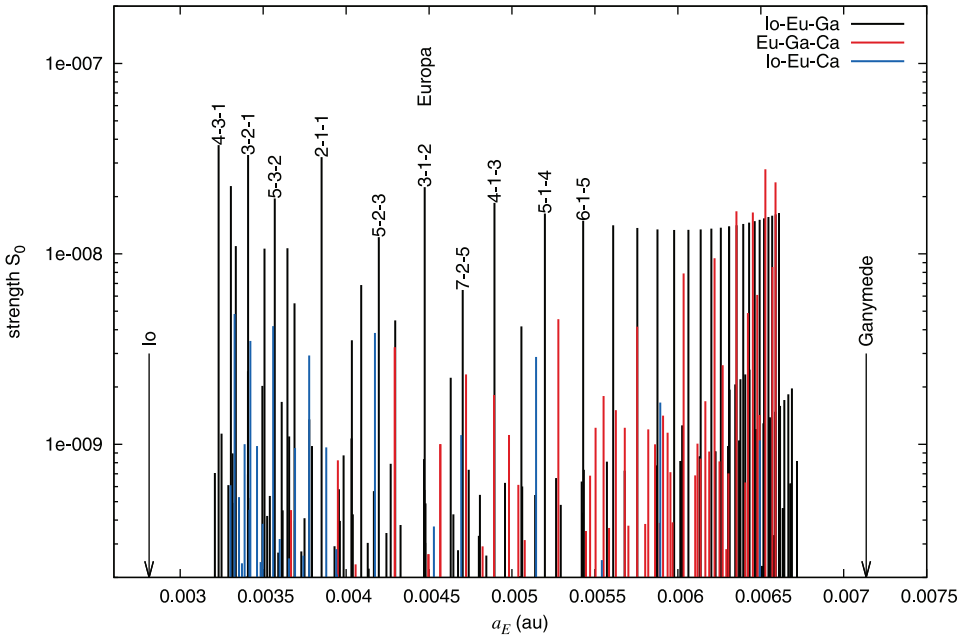

Fig. 17. Atlas of 3BRs between Io and Ganymede. Three body resonances involving Io-*Europa*-Ganymede in black, *Europa*-Ganymede-Callisto in red and Io-*Europa*-Callisto in blue where *Europa* is an hypothetical object with the same mass and orbital elements of the actual Europa but with a semimajor axis defined by the resonance. Some resonances involving Io-*Europa*-Ganymede are labeled. Positions of Io and Ganymede are indicated with arrows.

The method assumes there are no 2BRs between them, which it is not the case because of the existence of the resonance 2:1 between Io and Europa and also 2:1 between Europa and Ganymede. Then, the results we obtained for the 3BRs involving Io, Europa and Ganymede must be taken with caution. We started taking the two fixed bodies Io and Ganymede as P_1 and P_2 respectively, with its present orbits and masses taken from Table 2 and we calculated all relevant 3BRs located in between both satellites as experienced by a third body, P_0, with the same mass and orbital parameters of Europa, except for its semimajor axis which is defined by the different resonances we are trying to evaluate. The resulting set of resonances with their strengths is showed in Fig. 17 with black lines. As we expected, the actual Europa is located in the resonance $3E - 1I - 2G$, or $3 - 1 - 2$ in our notation, which is one of the strongest 3BRs of the system. Then, we repeated the method but considering Ganymede as P_1 and Callisto as P_2 and we calculate all relevant 3BRs involving these satellites with an hypothetical Europa. Finally, we repeat the procedure but taking Io as P_1 and Callisto as P_2. All three sets of 3BRs are plotted in Fig. 17. The resonance $3E - 1I - 2G$ is one of the strongest resonances located in a region relatively devoid of other perturbing 3BRs. It is possible to distinguish in the figure the second order 3BR $1E - 1I + 2G$ almost superimposed with $3E - 1I - 2G$ but with strength $S < 1 \times 10^{-9}$.

If we look at the ratios of the strengths that our method predicts for the resonance $3E - 1I - 2G$ we find $S_E/S_I \sim 6$ and $S_E/S_G \sim 12$ which can be compared with the ratios between the Δa obtained from the numerical integrations given, for example, in Musotto et al. (2002) which are $\Delta a_E/\Delta a_I \sim 4$ and $\Delta a_E/\Delta a_G \sim 6$. Note that in Musotto et al. (2002) a_I and a_G are evolving in phase while for the body in between, a_E, is shifted by half a libration period in agreement with Quillen (2011).

In order to distinguish the different resonances affecting Europa we have constructed dynamical maps for a simple model consisting of a system of the four satellites orbiting Jupiter with its orbital elements taken from Table 2 and considering Jupiter's oblateness through the J_2 term. The map for $\Delta\bar{a}$ in Fig. 18 top panel was constructed by means of numerical integrations for intervals of 15 years and using a moving window of 1 year to calculate $\bar{a}(t)$. The map is constructed with 10000 different initial conditions taken from a grid in (a, e) and we compared this map with the map obtained from the evolution of various critical angles. The dynamical map of Fig. 18 top panel shows with vivid colors large $\Delta\bar{a}$ associated with the borders of the resonance region and with dark colors small values of $\Delta\bar{a}$ associated with small amplitude librations in the center of the resonance or with no oscillations, typical of secular non resonant evolution outside the resonance. The maps for the critical angles show regions of small amplitude librations with dark colors and circulations with vivid colors. There is a close correlation between the dynamical map for $\Delta\bar{a}$ with the evolution of the critical angles $3\lambda_E - \lambda_I - 2\lambda_G$ of the 3BR, $2\lambda_E - \lambda_I - \varpi_E$ of the exterior 2BR $2E - 1I$ and $\lambda_E - 2\lambda_G + \varpi_E$ of the interior 2BR $1E - 2G$.

From examination of Fig. 18 we can conclude that the features in the map for $\Delta\bar{a}$ in the left region, between $a = 0.00444$ au

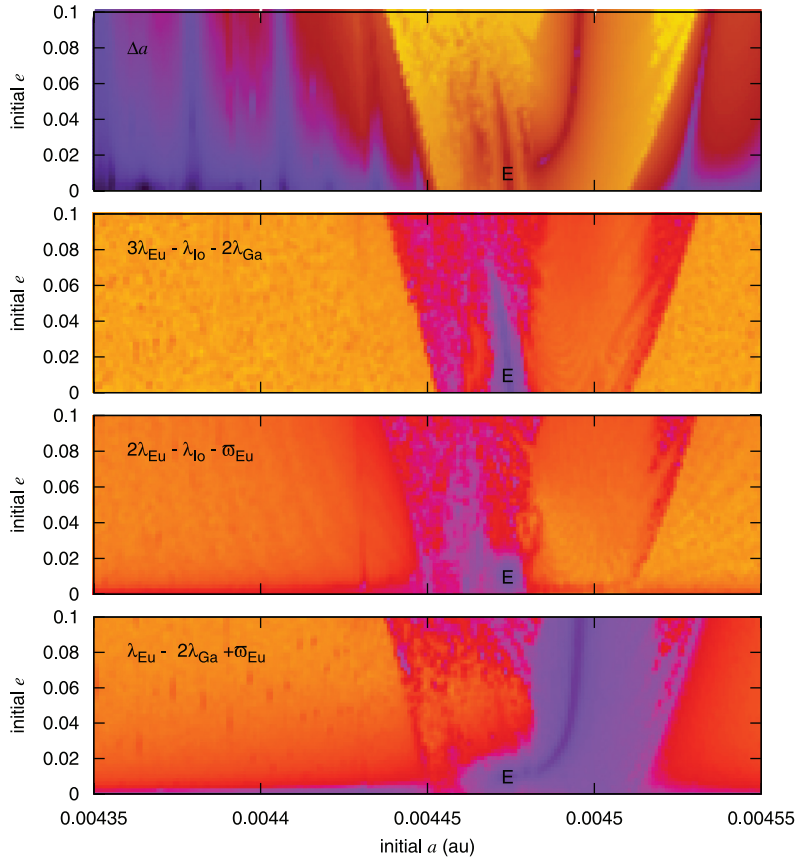

Fig. 18. Dynamical maps near the location of Europa, indicated with E. $\Delta\bar{a}$ in top panel is showed with dark regions corresponding to small amplitude (10^{-9} au) oscillations of a_0 and with vivid color regions corresponding to large amplitude (10^{-5} au) oscillations. The critical angles $3\lambda_E - \lambda_I - 2\lambda_G$ in second panel, $2\lambda_E - \lambda_I - \varpi_E$ in third panel and $\lambda_E - 2\lambda_G + \varpi_E$ in bottom panel. Dark colors correspond to small amplitude oscillations of the critical angles and vivid colors to large amplitude oscillations and circulations.

and $a = 0.00448$ au, have a very good match with the features in the map of the 3BR in Fig. 18 second panel. This map shows that Europa is located in the very central region of the 3BR, region which has low dependence with the eccentricity as is typical for a zero order 3BR. The zone at the right of $a = 0.00448$ au matches with the features in the map for the 2BR 2:1 between Europa and Ganymede at bottom panel in Fig. 18. In this panel it is possible to identify the Law of Structure of the resonance 2:1, which is the deviation of the location of the exact resonance from the nominal value a_{res} at low eccentricities as we have explained above. For completeness we show in the third panel the map for the corresponding critical angle for the exterior 2BR 1:2 between Io and Europa which seems to have no relevant effects in the map for $\Delta\bar{a}$. In our numerical integrations a particle with the same orbital elements of Europa shows librations in the three critical angles but the largest oscillations in a_E are correlated with the critical angle of the 3BR $3E - 1I - 2G$. Then, Fig. 18 suggests that Europa is mostly dominated by the pure 3BR.

Various attempts have been done in order to identify possible migrations of the Galilean satellites due to tidal effects caused by Jupiter and, consequently, to understand the future of the Laplacian resonance (Lainey et al., 2009). Fitting the parameters of a very complete physical model to a large set of astrometric positions Lainey et al. (2009) conclude that, due to the mechanism of tides in Jupiter-Io system, at present Io is migrating inwards to Jupiter at a very low rate ($\dot{a} \simeq -2.6 \times 10^{-14}$ au/yr) while Europa and Ganymede migrate outwards, being the system leaving the exact commensurability of the Laplacian resonance. In order to evaluate the strength of the Laplacian resonance and, in particular, if it is capable of surviving to a migration mechanism we performed a numerical simulation of the system given by Jupiter plus the four Galilean satellites with an imposed inwards migration for Io given by $\dot{a} = -1 \times 10^{-7}$ au/yr, that means approximately seven orders of magnitude greater than the deduced by Lainey et al. (2009). If the 3BR is not strong enough it will be broken by the imposed artificial migration, otherwise Europa and Ganymede will migrate in such a way that the resonant relation is conserved. The resulting evolution of the system is given in Fig. 19. In our simulation Europa responds migrating inwards like Io but Ganymede moves outwards; while Callisto does not experience orbital changes as is expected because it is not participating in the Laplacian resonant mechanism. All critical angles remain librating during the integration period but while the libration amplitude of the two 2BRs increase with time, the amplitude of the Laplacian resonance remains constant, see Fig. 19 bottom panel. Differences with results by Lainey et al. (2009) can be explained because the models are very different, but it is remarkable that in our experiment the 3BR persists. The largest amplitude oscillations in the three semimajor axes we see in Fig. 19 are linked to the librations of the Laplacian 3BR and the high frequency low amplitude oscillations are linked to the librations of $\lambda_E - 2\lambda_G + \varpi_E$, suggesting that the main dynamical mechanism is the 3BR and that the resonance $1E - 2G$ only makes a small contribution. This is consistent with the information we can deduce from Fig. 18. Our Io-migrating experiment does not pretend to show the actual dynamical evolution of the satellite system, just try to demonstrate that, even in case the 2BRs were breaking, the Laplacian 3BR is strong enough to survive, even imposing migration rates several order of magnitude greater than actual ones.

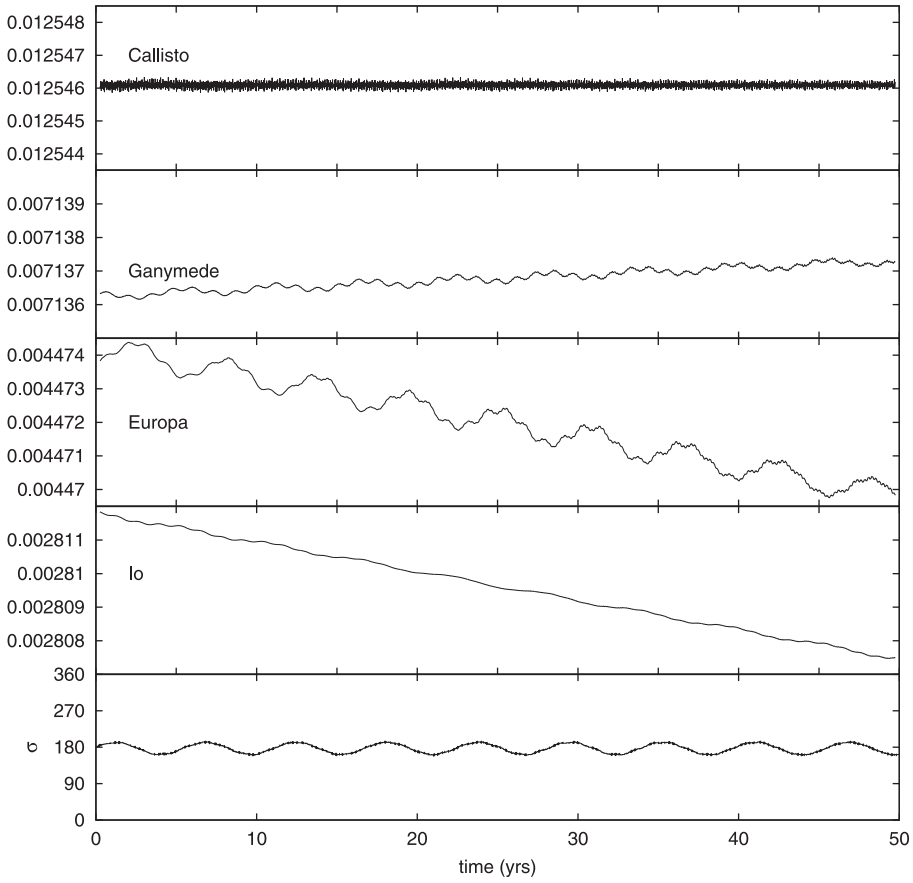

Fig. 19. Mean semimajor axes of Callisto, Ganymede, Europa and Io expressed in au evolving due to an induced arbitrary inwards migration of Io. Mean semimajor axes calculated using running window of 0.5 years. In bottom panel the corresponding evolution of the critical angle of the Laplacian resonance. The short period small amplitude oscillations in semimajor axes are correlated with the time evolution of the critical angle of the resonance $1E - 2G$.

4. Concluding remarks

Three body resonances between massive bodies generate different effects on each planet. The semianalytical method presented here have proven useful to predict the configurations and approximate strengths of the 3BRs generated by a system of three massive bodies with arbitrary orbits which are not in 2BRs between them and provides a useful tool for evaluating the dynamical relevance of 3BRs among planetary and satellite systems. It allows to analyze the dependence of the strengths on each planet with the masses, eccentricities and inclinations of all involved planets. In particular, the dependence with the inclinations can now be explored for the first time. For near zero eccentricity orbits, zero order 3BRs are the strongest ones, even stronger than 2BRs in some cases. On the other hand, for excited systems, first or second order 3BRs could be equally relevant than zero order 3BRs, but if 2BRs are present in the neighborhood they will dominate. When we compared the effect on each planet participating in a resonance, the most affected one is that of smallest mass or, in general, the planet in the middle when the masses are similar. We confirmed that the planet in the middle has oscillations in a shifted half a libration period with respect to the other planets. It is common that in a migrating scenario one of the bodies locked in a pure 3BR migrate in the opposite direction than the other two due to the existence of a new degree of freedom in the equation linking the mean motions. Our very preliminary results of our numerical simulations suggest that capture in a pure 3BR is an unusual event but, on the other hand, systems captured in pure 3BRs can survive to imposed migration mechanisms. Our study of the case of the Galilean satellites suggest that the Laplacian 3BR dominate the system and is strong enough to maintain the system locked in resonance even for migration rates several orders of magnitude greater than the deduced by present theories.

Acknowledgments

We acknowledge support from PEDECIBA and Project CSIC Grupo I+D 831725 - Planetary Sciences. We thank the reviewers that contributed to clarify various points of the original manuscript.

Appendix A. Numerical approximation to the disturbing function for planetary three body resonances

Given two planets P_1 and P_2 in arbitrary orbits, the mean resonant disturbing function, $\mathcal{R}(\sigma)$, that drives the resonant motion of the planet P_0 assumed inside an arbitrary 3BR could be ideally calculated eliminating the short period terms of the resonant disturbing function R for the planet by means of

$$\mathcal{R}(\sigma) = \frac{1}{4\pi^2}\int_0^{2\pi} d\lambda_1 \int_0^{2\pi} R\Big(\lambda_0(\sigma, \lambda_1, \lambda_2, \gamma), \lambda_1, \lambda_2\Big) d\lambda_2 \quad \text{(A.1)}$$

where λ_0 was explicitly written in terms of the variables λ_1, λ_2 and the parameters σ, γ using Eq. (4) and where $R(\lambda_0, \lambda_1, \lambda_2) = R_{01} + R_{02}$ being

$$R_{ij} = k^2 m_j \left(\frac{1}{r_{ij}} - \frac{\vec{r_i}\cdot\vec{r_j}}{r_j^3}\right) \quad \text{(A.2)}$$

where k is the Gaussian constant, m_j the mass of planet P_j and $\vec{r_i}, \vec{r_j}$ are the astrocentric positions of bodies with subindex i and j

respectively. Note that for each set of values $(\sigma,\ \lambda_1,\ \lambda_2,\ \gamma)$ there are k_0 values of λ_0 that satisfy Eq. (4), which are:

$$\lambda_0 = (\sigma - k_1\lambda_1 - k_2\lambda_2 - \gamma)/k_0 + n2\pi/k_0 \tag{A.3}$$

with $n = 0, 1, \ldots, k_0 - 1$. All them contribute to $\mathcal{R}(\sigma)$ in Eq. (A.1) so we have to evaluate all these k_0 terms and calculate the mean, which is equivalent to integrate in λ_0 maintaining the condition (4).

The disturbing function of a 3BR is a second order function of the planetary masses, which means the calculation of the double integral (A.1) cannot be done over the perturbing function evaluated at the unperturbed astrocentric positions. To properly evaluate the integral it is necessary to take into account their mutual perturbations in the position vectors $\vec{r_i}$. Two body mean motion resonances are a simpler case because being a first order perturbation in the planetary masses the position vectors can be substituted by the Keplerian, non perturbed positions.

In order to estimate the behavior of $\mathcal{R}(\sigma)$, Gallardo (2014) adopted the following scheme for computing the double integral of Eq. (A.1):

$$R(\lambda_0, \lambda_1, \lambda_2) \simeq R_u + \Delta R \tag{A.4}$$

where R_u stands from R calculated at the unperturbed positions of the three bodies and ΔR stands from the variation in R_u generated by the perturbed (not Keplerian) displacements of the three bodies in a small interval Δt. More clearly, given any set of the three position vectors $\vec{r_i}$ satisfying Eq. (4) we compute the mutual perturbations of the three bodies and calculate the $\Delta\vec{r_i}$ that they generate in a small interval Δt and the ΔR associated. This scheme is equivalent to evaluate the integral over the infinitesimal trajectory the system follows due to the mutual perturbations when released at all possible unperturbed positions that verify Eq. (4). We have then

$$R_u = R_{01} + R_{02} \tag{A.5}$$

$$\Delta R = \Delta R_{01} + \Delta R_{02} \tag{A.6}$$

where R_{01} and R_{02} refer to the disturbing functions evaluated at the unperturbed positions and ΔR_{01} and ΔR_{02} refer to the variations due to displacements caused by the mutual perturbations:

$$\Delta R_{01} = \nabla_0 R_{01}\Delta\vec{r_0} + \nabla_1 R_{01}\Delta\vec{r_1} \tag{A.7}$$

$$\Delta R_{02} = \nabla_0 R_{02}\Delta\vec{r_0} + \nabla_2 R_{02}\Delta\vec{r_2} \tag{A.8}$$

where $\Delta\vec{r_i}$ refers to displacements with respect to the astrocentric Keplerian motion and being

$$\nabla_i R_{ij} = k^2 m_j\left(\frac{\vec{r_j} - \vec{r_i}}{r_{ij}^3} - \frac{\vec{r_j}}{r_j^3}\right) \tag{A.9}$$

$$\nabla_j R_{ij} = k^2 m_j\left(\frac{\vec{r_i} - \vec{r_j}}{r_{ij}^3} - \frac{\vec{r_i}}{r_j^3} + 3(\vec{r_i}\vec{r_j})\frac{\vec{r_j}}{r_j^5}\right) \tag{A.10}$$

From the equations of motion we have:

$$\Delta\ddot{\vec{r}}_0 = \nabla_0 R_{01} + \nabla_0 R_{02} \tag{A.11}$$

$$\Delta\ddot{\vec{r}}_1 = \nabla_1 R_{12} + \nabla_1 R_{10} \tag{A.12}$$

$$\Delta\ddot{\vec{r}}_2 = \nabla_2 R_{21} + \nabla_2 R_{20} \tag{A.13}$$

Integrating twice we obtain the displacements with respect to the Keplerian motion:

$$\Delta\vec{r}_0 \simeq (\nabla_0 R_{01} + \nabla_0 R_{02})\frac{(\Delta t)^2}{2} \tag{A.14}$$

$$\Delta\vec{r}_1 \simeq (\nabla_1 R_{12} + \nabla_1 R_{10})\frac{(\Delta t)^2}{2} \tag{A.15}$$

$$\Delta\vec{r}_2 \simeq (\nabla_2 R_{21} + \nabla_2 R_{20})\frac{(\Delta t)^2}{2} \tag{A.16}$$

As the integral of $R_u = R_{01} + R_{02}$ becomes independent of σ, we are only interested in computing the function $\rho(\sigma)$ defined by

$$\rho(\sigma) = \frac{1}{4\pi^2}\int_0^{2\pi} d\lambda_1 \int_0^{2\pi} \Delta R d\lambda_2 \tag{A.17}$$

always satisfying Eq. (4). Its dimensions are $[M]^2k^2/[L]$ in solar masses, au and days.

Note that $\rho(\sigma)$ is a summation of terms each one factorized by two masses while in the case of 2BRs the disturbing function is proportional to only one planetary mass, making 3BRs much weaker than 2BRs. Note also that ΔR is calculated via some arbitrary Δt that we identify with the permanence time in each element of the phase space $(\Delta\lambda_0,\ \Delta\lambda_1,\ \Delta\lambda_2)$. If the double integral is computed dividing the dominium in N equal steps in λ_1 and N equal steps in λ_2 we can calculate the mean elapsed time Δt in the element of phase space as

$$\Delta t = \frac{\sqrt[3]{T_0 T_1 T_2}}{N} \tag{A.18}$$

where T_i are the orbital periods. Another way of understanding the meaning of Δt is to calculate the probability of finding the system in a particular configuration during Δt, which is $(\Delta t)^3/(T_0T_1T_2)$. Then

$$\Delta t^2 = \frac{4\pi^2 a_0 a_1 a_2}{k^2 M N^2} \tag{A.19}$$

where M is the mass of the central body (star or planet) expressed in solar masses. Note that N is an arbitrary integer but it must be always the same if we want to compare functions $\rho(\sigma)$ for different resonances. Taking N equal for all resonances its actual value is irrelevant; in our codes we use $N = 1$. Considering σ as a constant parameter we calculate the integral (A.17) for a set of values of σ between $(0,\ 2\pi)$ and we obtain numerically $\rho(\sigma)$.

We consider the strength of the resonance, S, the value of the semiamplitude $S = \Delta\rho/2$ as in Gallardo (2014). The reason for this definition is that if σ generates large variations in ρ is because it has some dynamical relevance. On the other hand, if variations in ρ are negligible is because the critical angle, that means the resonance, is irrelevant for the dynamics.

An important difference with the restricted case is that in the general 3BR problem all three planets feel the resonance, then there are dynamical effects in all three planets. We calculate these resonant effects in the other two planets following an analogue procedure than the one we followed for planet P_0. While Eqs. (A.14)–(A.16) are the same the corresponding ΔR are for planet P_1:

$$\Delta R = \Delta R_{10} + \Delta R_{12} \tag{A.20}$$

and for planet P_2:

$$\Delta R = \Delta R_{20} + \Delta R_{21} \tag{A.21}$$

where

$$\Delta R_{10} = \nabla_1 R_{10}\Delta\vec{r_1} + \nabla_0 R_{10}\Delta\vec{r_0} \tag{A.22}$$

$$\Delta R_{12} = \nabla_1 R_{12}\Delta\vec{r_1} + \nabla_2 R_{12}\Delta\vec{r_2} \tag{A.23}$$

and

$$\Delta R_{20} = \nabla_2 R_{20}\Delta\vec{r_2} + \nabla_0 R_{20}\Delta\vec{r_0} \tag{A.24}$$

$$\Delta R_{21} = \nabla_2 R_{21}\Delta\vec{r_2} + \nabla_1 R_{21}\Delta\vec{r_1} \tag{A.25}$$

We finally obtain the three strengths S_0, S_1, S_2 for the three planets:

$$S_i = (\rho_{max} - \rho_{min})/2 \tag{A.26}$$

The strengths S_i as defined above must have some relation, not necessarily linear, with the dynamical effects of the resonance on P_i, for example, the width of the resonance or the amplitude Δa_i of the librations observed in the semimajor axis of P_i. The code for this algorithm can be downloaded from www.fisica.edu.uy/~gallardo/atlas.

References

Aksnes, K., 1988. General formulas for three-body resonances. In: NATO Advanced Study Institute on Long-Term Dynamical Behaviour of Natural and Artificial N–Body Systems, pp. 125–139.

Batygin, K., 2015. Capture of planets into mean-motion resonances and the origins of extrasolar orbital architectures. Mon. Not. R. Astron. Soc. 451, 2589–2609.

Batygin, K., Deck, K.M., Holman, M.J., 2015. Dynamical evolution of multi-resonant systems: The case of GJ876. Astron. J. 149 (5), 167.

Batygin, K., Morbidelli, A., 2013. Dissipative divergence of resonant orbits. Astron. J. 145 (1), 1.

Callegari Jr., N., Yokoyama, T., 2010. Numerical exploration of resonant dynamics in the system of saturnian major satellites. Planet. Space Sci. 58, 1906–1921.

Fabrycky, D.C., Lissauer, J.J., Ragozzine, D., et al., 2014. Architecture of Kepler's multi-transiting systems II. New investigations with twice as many candidates. Astrophys. J. 790, 146.

Fernández, J.A., Gallardo, T., Brunini, A., 2002. Are there many inactive jupiter family comets among the near-Earth asteroid population? Icarus 159, 358–368.

Ferraz-Mello, S., 1979. Dynamics of the Galilean Satellites. An Introductory Treatise. USP - IAG.

Ferraz-Mello, S., 1988. The high eccentricity librations of the hildas. Astron. J. 96, 400–408.

Gallardo, T., 2006. Atlas of mean motion resonances in the Solar System. Icarus 184, 29–38.

Gallardo, T., 2014. Atlas of three body mean motion resonances in the Solar System. Icarus 231, 273–286.

Gomes, G., 2012. Ressonâncias de Três Corpos: Estudo da Dinâmica da Zona Habitável do Sistema Exoplanetário GJ581. USP Ph.d thesis.

Guzzo, M., 2005. The web of three-planet resonances in the outer Solar System. Icarus 174, 273–284.

Guzzo, M., 2006. The web of three-planet resonances in the outer Solar System II. a source of orbital instability for uranus and neptune. Icarus 181, 475–485.

Lainey, V., Arlot, J.-E., Karatekin, Ö., et al., 2009. Strong tidal dissipation in io and jupiter from astrometric observations. Nature 459, 957.

Lazzaro, D., Ferraz-Mello, S., Veillet, C., 1984. The laplacian resonance amongst uranian inner satellites. Astron. Astrophys. 140, 33–38.

Libert, A.S., Tsiganis, K., 2011. Trapping in three-planet resonances during gas-driven migration. Celest. Mech. Dynam. Astron. 111, 201–218.

Malhotra, R., 1991. Tidal origin of the laplace resonance and the resurfacing of ganymede. Icarus 94, 399–412.

Martí, J.G., Giuppone, C.A., Beaugé, C., 2013. Dynamical analysis of the gliese-876 laplace resonance. Mon. Not. R. Astron. Soc. 433, 928–934.

Musotto, S., Moore, W., Schubert, G., 2002. Numerical simulations of the orbits of the galilean satellites. Icarus 504, 500–504.

Nesvorný, D., Morbidelli, A., 1999. An analytic model of three-body meanmotion resonances. Celest. Mech. Dynam. Astron. 71, 243–271.

Papaloizou, J., 2015. Three body resonances in close orbiting planetary systems: tidal dissipation and orbital evolution. Int. J. Astrobiol. 14, 291–304.

Peale, S.J., Lee, M.H., 2002. A primordial origin of the laplace relation among the galilean satellites. Science 298 (5593), 593–597.

Quillen, A.C., 2011. Three-body resonance overlap in closely spaced multiple-planet systems. Mon. Not. R. Astron. Soc. 418, 1043–1054.

Quillen, A.C., French, R.S., 2014. Resonant chains and three-body resonances in the closely packed inner uranian satellite system. Mon. Not. R. Astron. Soc. 445 (4), 3959–3986.

Showalter, M.R., Hamilton, D.P., 2015. Resonant interactions and chaotic rotation of plutoÆs small Moons. Nature 522 (7554), 45–49.

Showman, A., Malhotra, R., 1997. Tidal evolution into the laplace resonance and the resurfacing of ganymede. Icarus 127 (1), 93–111.

Showman, A.P., Stevenson, D.J.D., Malhotra, R., 1997. Coupled orbital and thermal evolution of ganymede. Icarus 192, 367–383.

Sinclair, A.T., 1975. The orbital resonance amongst the galilean satellites of jupiter. Mon. Not. R. Astron. Soc. 12, 89–96.

Smirnov, E.A., Shevchenko, I.I., 2013. Massive identifcation of asteroids in three-body resonances. Icarus 222, 220–228.